Proc. Natl. Acad. Sci. USA
Vol. 91, pp. 9072–9076, September 1994
Neurobiology

Transgenic engineering of neuromuscular junctions in *Xenopus laevis* embryos transiently overexpressing key cholinergic proteins

(acetylcholinesterase cytochemistry/nicotinic muscle acetylcholine receptor/electron microscopy/posttranscriptional regulation/synaptic targeting)

MICHAEL SHAPIRA*, SHLOMO SEIDMAN*, MEIRA STERNFELD*, RINA TIMBERG*, DANIELA KAUFER*, JAMES PATRICK†, AND HERMONA SOREQ*‡

*Department of Biological Chemistry, The Institute of Life Sciences, The Hebrew University, Jerusalem 91904, Israel; and †Baylor College of Medicine, Division of Neuroscience, One Baylor Plaza, Houston, TX 77030-3498

Communicated by Jean-Pierre Changeux, April 18, 1994

ABSTRACT **To examine the role of key cholinergic proteins in the formation of neuromuscular junctions (NMJs), we expressed DNAs encoding the mouse muscle nicotinic acetylcholine receptor (nAChR) or human brain and muscle acetylcholinesterase (hAChE) in developing *Xenopus laevis* embryos. Acetylthiocholine hydrolysis and α-bungarotoxin binding in homogenates of transgenic embryos revealed transient overexpression of the respective proteins for at least 4 days postfertilization. Moreover, hAChE injection induced an ≈2-fold increase in endogenous *Xenopus* nAChR. Electron microscopy coupled with cytochemical staining for AChE activity revealed that AChE-stained areas, which reached 0.17 μm² in NMJs of control embryos raised at 21°C, increased up to 0.53 and 0.60 μm² in nAChR and hAChE transgenics, respectively. These increases coincided with the appearance of a class of large NMJs with average postsynaptic lengths up to 1.8-fold greater than controls. As much as 57% and 34% of the NMJs in animals transgenic for nAChR and hAChE, respectively, displayed AChE activity in nerve terminals in addition to muscle labeling, as compared with 10% nerve-labeled NMJs in control animals. Moreover, area, but not length values, were >2-fold larger in hAChE-expressing NMJs labeled in their nerve terminals than in those labeled in muscle alone, reflecting a hAChE-induced increase in synaptic cleft width. These findings indicate that modulation of cholinergic neurotransmission in NMJs modifies the features of nerve–muscle connections.**

The role of acetylcholine (ACh) as a neurotransmitter has long been established (reviewed in ref. 1). However, many basic and clinical problems associated with the function of ACh in neuromuscular junctions (NMJs) remain unresolved (2). These include possible trophic effects exerted by ACh on NMJ development and cholinergic neurotransmission (3). Structural alterations observed in NMJs of patients suffering cholinergic deficits (4) are consistent with the hypothesis that ACh, like some other neurotransmitters (5), operates as a morphogenic factor. A trophic function for ACh could partially account for neuronal induction of developmental changes in muscle gene expression (6). Thus, the concerted expression and localization of numerous pre- and postsynaptic proteins (7), a prerequisite for the creation and maintenance of a functional NMJ, could be coordinated, in part, by ACh.

A morphogenic role for ACh implies a direct or indirect function(s) for cholinergic proteins in NMJ development. Furthermore, balanced functioning of the NMJ should require coordinated regulation of ACh-associated proteins. Indeed, accumulated evidence indicates coordinated expression of proteins associated with cholinergic neurotransmission in NMJs: (*i*) the nematode *unc17* gene encoding the vesicular ACh transporter shares a common promoter with the choline acetyltransferase gene (8), (*ii*) avian embryos in which cholinergic neurotransmission is blocked by organophosphates develop neuromuscular deformities (9), and (*iii*) certain patients with congenital myasthenias suffer deficiencies in both the muscle nicotinic ACh receptor (nAChR) and the ACh hydrolyzing enzyme acetylcholinesterase (AChE), although neither of these proteins is apparently mutated (4).

To investigate the role of cholinergic neurotransmission in NMJ formation, we initiated studies to experimentally modulate the levels of AChE or nAChR during synaptogenesis in transiently transgenic embryos of *Xenopus laevis*. Overexpression of AChE in developing *Xenopus* embryos injected with DNA constructs carrying the human *ACHE* gene (hAChE) caused ultrastructural changes in NMJs (10, 11). Yet, it remained unclear whether these changes reflected a response to altered ACh metabolism and whether such responses could be induced by changes in the expression of other cholinergic proteins. To perform the reciprocal experiment, we coinjected four plasmids encoding the individual subunits of mouse muscle nAChR (12). Our findings reveal that overexpression of either AChE or AChR induces pronounced alterations in NMJ ultrastructure and strengthen the evidence implying a role for cholinergic neurotransmission in NMJ biogenesis.

MATERIALS AND METHODS

In vitro fertilization and microinjection of *X. laevis* eggs were performed as described (10, 11). Fertilized eggs were injected with ≈1 ng of DNA (AChE DNA ligated to the cytomegalovirus enhancer-promoter region; refs. 10 and 11) encoding brain and muscle AChE or with pooled DNAs encoding the individual subunits of the *Xenopus*-expressible (13) mouse nAChR in a ratio of 2:1:1:1 ($\alpha/\beta/\gamma/\delta$; Fig. 1). Injections were performed within the first three cleavage cycles and embryos were cultured for 1–6 days postfertilization at 21°C.

Biochemical measurements of nAChR were performed with biotinylated α-bungarotoxin (α-Bgt) (ref. 14; see legend to Fig. 2).

Biochemical analyses of AChE activities were performed as detailed elsewhere (15), as were cytochemical staining and electron microscopy analyses (10, 11). Morphometric analyses were performed with the SIGMASCAN software (Jandel, Corte Madera, CA) or the Magicscan image analysis microscope controller (Applied Imaging International, Dukesway, U.K.) on micrographed NMJ structures.

The publication costs of this article were defrayed in part by page charge payment. This article must therefore be hereby marked "*advertisement*" in accordance with 18 U.S.C. §1734 solely to indicate this fact.

Abbreviations: ACh, acetylcholine; AChE, acetylcholinesterase; hAChE, human AChE; α-Bgt, α-bungarotoxin; nAChR, muscle nicotinic ACh receptor; NMJ, neuromuscular junction.

‡To whom reprint requests should be addressed.

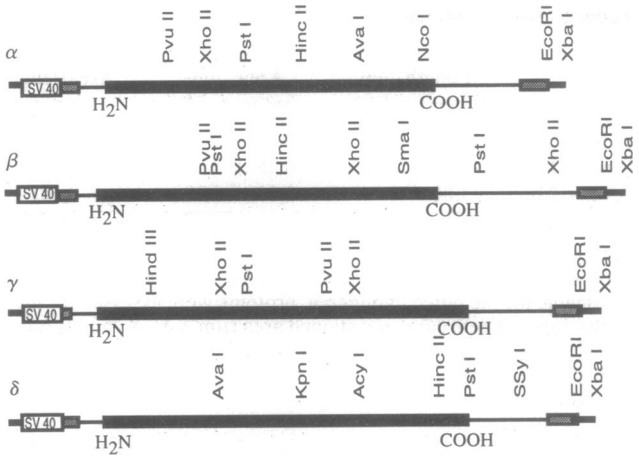

FIG. 1. DNA constructs encoding the subunits of the mouse muscle nAChR. cDNA clones encoding the subunits of mouse muscle nAChR (13) were removed from vector pSP65 and placed in pcDNA I (12) using the restriction sites indicated. Heavy line, portion of the clone encoding the mature subunit; shaded box, multiple cloning site of pcDNA I. Simian virus 40 (SV40) promoter is shown as the box to the left of the *Hin*dIII cloning site.

RESULTS

We used microinjection of plasmid vectors encoding the "tailed" (T) form of hAChE (10, 11) or mouse muscle nAChR (Fig. 1) to induce ectopic overexpression of the corresponding proteins during NMJ formation in developing *Xenopus* embryos. Homogenates from embryos injected with the receptor-encoding plasmids displayed increased α-Bgt binding as compared with control uninjected embryos (Fig. 2*A Left*). This increase diminished after day 3 postfertilization—a transient pattern of overexpression resembling that observed for hAChE in *Xenopus* embryos (ref. 11; Fig. 2*B Right*). Interestingly, homogenates of embryos overexpressing hAChE also displayed increased α-Bgt binding (Fig. 2*A Right*). However, expression of endogenous *Xenopus* AChE, as measured in homogenates, was unaffected by nAChR overexpression (Fig. 2*B Left*).

Cytochemical staining of AChE and nAChR in cultured myotomal cells from the transgenic embryos demonstrated that overexpression occurred, at least in part, in muscle cells (results not shown). To search for specific changes in NMJ structure and in synaptic AChE levels, electron microscopy coupled with cytochemical activity staining (10, 11) was performed. Conspicuous differences were observed in the pre- and postsynaptic lengths of NMJs from embryos transgenic for either hAChE or nAChR as compared to uninjected controls. NMJs from control embryos 2 days postfertilization were relatively short, exhibited narrow synaptic clefts, and displayed limited deposition of the crystalline reaction product indicative of AChE activity (Fig. 3*A*). In embryos transgenic for either nAChR (Fig. 3*B*) or hAChE (Fig. 3*C*), nerve terminals were clustered and synaptic clefts appeared enlarged, displaying abundant dense deposits of AChE reaction products.

Morphometric measurements revealed that synapses from 2-day-old animals transgenic for mouse nAChR featured, on average, somewhat larger postsynaptic membranes and 2.25-fold larger cross sections stained for AChE activity than NMJs from control animals (Table 1; $P < 0.05$; Student's t test). The average postsynaptic length measured for NMJs from animals transgenic for hAChE was 1.8-fold larger than that determined for controls, and AChE accumulation in these NMJs was 4-fold higher than that observed in uninjected embryos (Table 1; $P < 0.001$). The ratio of stained area to NMJ length was ≈2-fold higher in animals transgenic for nAChR as compared to controls, whereas NMJs from hAChE transgenics displayed an almost 3-fold increase in this ratio (Table 1).

As few as 10% of the NMJs in uninjected embryos developed to the length of 3.5 μm (Fig. 4*A*). In embryos transgenic for nAChR, ≈30% of the NMJs were 3.5–5.5 μm long. In animals transgenic for hAChE, 50% of the NMJs reached lengths of 3.5–6.5 μm. A direct relationship was observed between area stained for AChE activity and postsynaptic length in all groups, indicating that the capacity of NMJs to accommodate either the *Xenopus* or the human enzyme increased with length (Fig. 4*B*). Nevertheless, within most of the length, groups average stained areas were considerably greater in NMJs from embryos transgenic for hAChE than in those from controls or from those overexpressing nAChR (Fig. 4*B*).

The transient expression of heterologous genes in DNA-microinjected *Xenopus* embryos is known to be mosaic (16). To discriminate between NMJs that overexpressed the transgenes and those that did not, we searched for a cytochemical marker. To this end, we analyzed NMJs stained for AChE

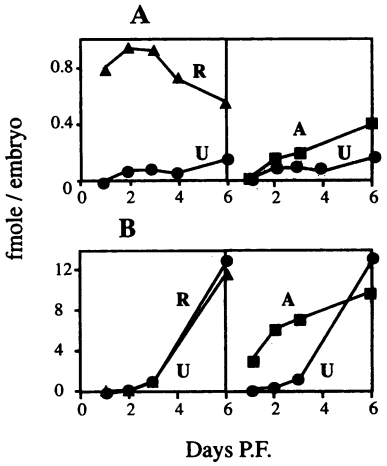

FIG. 2. Transgenic and induced overexpression of key cholinergic proteins in *Xenopus* embryo homogenates. *Xenopus* embryo microinjection with the noted plasmid DNAs was as described. (*A*) α-Bgt binding levels. Ten embryos at different developmental stages were harvested in groups of 6–10 and stored frozen until use. Homogenates were prepared in 50 mM Tris·HCl, pH 7.6/0.5% Triton X-100/1 mM EDTA/1 mM EGTA/0.1 mM phenylmethylsulfonyl fluoride/0.1 unit of aprotinin per ml (Sigma) (50 μl per embryo). After 90 min of incubation at room temperature and 15 min of centrifugation (Eppendorf), supernatants were diluted 1:20 in 0.1 M carbonate/bicarbonate buffer (pH 9.5). Samples (200 μl) were added to Maxisorp Immunoplates (Nunc) and incubated overnight at 4°C. Plates were washed (2 min; three times) with 20 mM Tris·HCl buffer (pH 7.6) containing 137 mM NaCl, 0.1% Tween 20, and 1 mg of bovine serum albumin (BSA) per ml (washing buffer). BSA (10 mg/ml) was added for 40 min at room temperature to block nonspecific binding. After washing, biotinylated α-Bgt (Molecular Probes) was added (2 μg/ml in washing buffer; 150 μl per well; 3 hr at room temperature). Unbound toxin was washed away as described above and ExtrAvidin alkaline phosphatase conjugate was added (Sigma; 1:10,000 dilution in washing buffer; 150 μl per well; 90 min at room temperature). Plates were washed twice as described above and then twice with 10 mM diethanolamine buffer containing 5 mM $MgCl_2$ (pH 9.5). 2-(*p*-Nitrophenyl) phosphate (1 mg/ml) in the diethanolamine buffer was added for 1 hr and colored reaction product was monitored in a V_{max} kinetic microplate reader (Molecular Devices; 405 nm) equipped with the SOFTMAX program for automated determination of hydrolysis rates. Calculations of receptor quantities in fmol of protein per embryo were performed as detailed elsewhere (11). (*B*) AChE levels. Activities were determined by measuring acetylthiocholine hydrolysis (11). Letters above the curves represent the DNA construct injected. U, uninjected control embryos; A, embryos injected with the hAChE construct (10, 11); R, coinjection of four plasmids encoding the pentameric mouse muscle nicotinic receptor (12, 14). P.F., postfertilization.

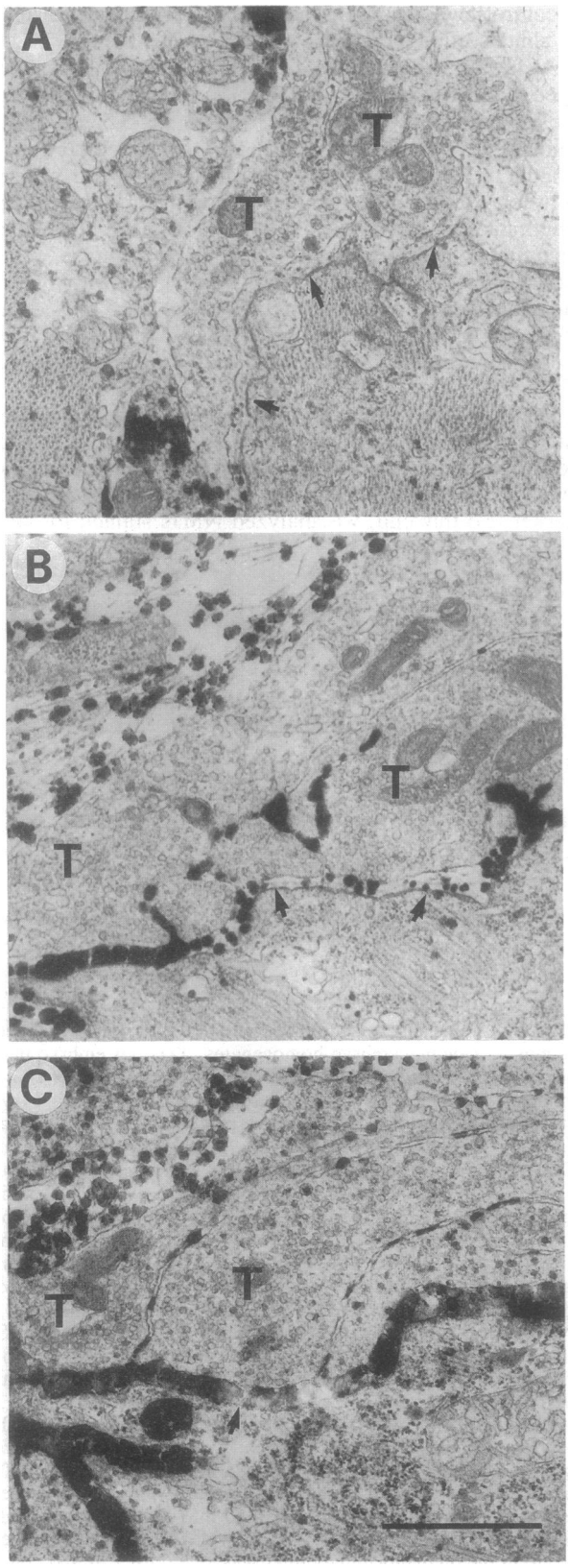

FIG. 3. Ultrastructural alterations of NMJ in transiently transgenic *Xenopus* embryos. Electron microscopy of NMJ structures in cross sections from 2-day-old *Xenopus* embryos grown at 21°C was performed as described. Representative micrographs of NMJs (arrows) from uninjected (*A*), nAChR- (*B*), and hAChE- (*C*) overexpressing embryos are shown. T, nerve terminal. Note expanded NMJs from embryos transgenic for either the muscle AChE form or for nAChR and the overexpression of AChE in both types of the transgenic NMJs. (Bar = 1 μm.)

Table 1. Structural features and AChE activities of NMJs from *Xenopus* embryos expressing nAChR or hAChE

Group	Length, μm (mean ± SD)	Area, μm² (mean ± SD)	Area/length, ratio
U (n = 21)	2.16 ± 1.31	0.08 ± 0.09	0.037
R (n = 22)	2.70 ± 1.22	0.18 ± 0.15*	0.067
A (n = 23)	3.80 ± 2.14	0.33 ± 0.29	0.087

AChE cytochemical staining and electron microscopy were as detailed elsewhere (10, 11). Micrographs of the indicated numbers (n) of cross sections of NMJ structures from 2-day-old *Xenopus* embryos transgenic for the noted cholinergic proteins were assessed for mean postsynaptic length (μm) and stained area (μm²). U, A, and R reflect NMJs from uninjected and hAChE- and nAChR-overexpressing embryos, respectively.
*n = 14.

activity in their nerve terminals separately from those in which nerve terminals were unstained. The fraction of nerve-labeled NMJs increased from 10% (2/21) in control embryos to 57% (8/14) in embryos overexpressing nAChR and 34% (8/23) in those transgenic for hAChE (Fig. 5*A*). Thus, the expression of endogenous *Xenopus* AChE and/or exogenous hAChE was enhanced in part of the nerve terminals of transgenic embryos. Therefore, most of the nerve-labeled NMJs in both experimental groups could be regarded as expressing the heterologous transgenes.

Significantly increased synaptic AChE staining was observed in NMJs from hAChE-injected embryos in which nerve terminals were labeled as compared with unlabeled NMJs (Fig. 5*B*). However, the neuronal overexpression of hAChE did not affect postsynaptic length (Fig. 5*C*). Therefore, this increase in stained areas apparently reflected widening of synaptic clefts. Fig. 5 *D* and *E* illustrates the qualitative difference between a NMJ in which AChE expression is limited to muscle (Fig. 5*E*) and a NMJ in which esterase expression is seen in both nerve and muscle (Fig. 5*D*), with prominent widening of the synaptic cleft in the neuron-expressing NMJ. In contrast, there was no difference between nerve-stained and unstained NMJs with regard to

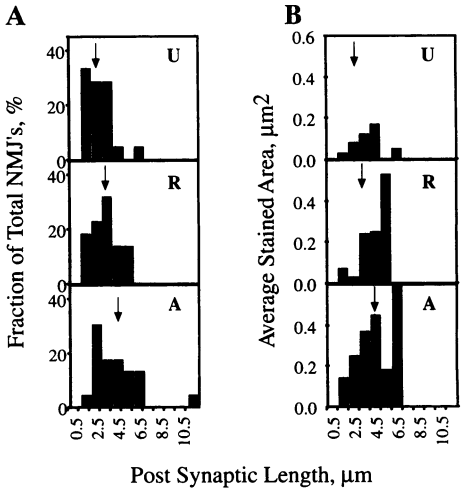

FIG. 4. Size and staining distributions in transgenic NMJs. (*A*) Length distribution. Electron microscopy was as detailed elsewhere (10, 11). Micrographs of randomly selected NMJ structures from 2-day-old *Xenopus* embryos from three different experiments, transgenic for the noted cholinergic proteins and raised at 21°C, were evaluated for postsynaptic length. Bars represent fraction of total NMJs analyzed (n = 21–23). Arrows denote weighted average length in each experimental system. (*B*) AChE activity staining distribution. Experimental details were as described in *A*. Cytochemical staining for AChE activity was performed as detailed elsewhere (11). Average stained areas are presented as a function of length.

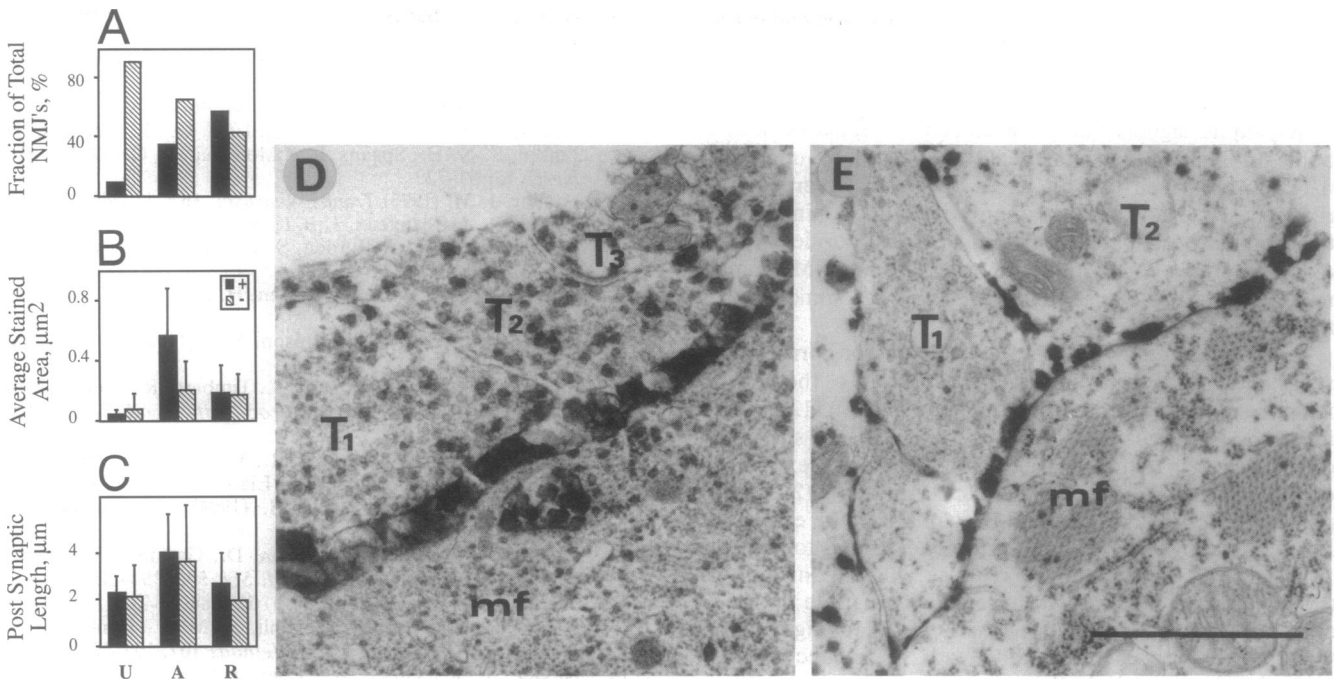

FIG. 5. AChE expression in nerve terminals increases stained areas but not postsynaptic lengths of NMJs. (*A*) Enhanced AChE expression in nerve terminals from transgenic embryos. Bars represent fractions of nerve terminals stained (+) or unstained (−) for AChE activity of total (*n*) synapses measured. Experimental data were as in Fig. 4*B*. Note the small fraction of stained nerve terminals in synapses of uninjected embryos (U; $n = 21$) as compared to the higher values in those transgenic for hAChE (A; $n = 23$) or nAChR (R; $n = 22$). (*B*) Increased AChE staining in the synaptic cleft of neuron-expressing transgenic NMJs. Values are presented as average stained area (μm^2) per NMJ. Note significant difference between values in synapses of hAChE-injected embryos (*A*) stained at the nerve terminal (+) and those that were not (−). In these measurements, $n = 14$ for AChR transgenics. (*C*) Terminal labeling does not alter postsynaptic length. No significant differences in postsynaptic length were observed between NMJs with stained (+) or unstained (−) terminals in the three experimental groups. (*D* and *E*) Representative micrographs of NMJs from embryos overexpressing hAChE. Experimental procedures and embryos are the same as in Fig. 4*B*. Note the wider synaptic cleft in the NMJ stained for AChE activity in the nerve terminal (*D*) as compared with the unstained one (*E*). T, nerve terminal; mf, muscle fiber. (Bar = 1 µm.)

AChE-stained area in either control embryos or those transgenic for nAChR (Fig. 5*B*). This demonstrated that the neuronal input of *Xenopus* AChE to the synaptic cleft is subject to more rigid control than that operating on the heterologous human enzyme.

DISCUSSION

We observed ultrastructural changes in neuromuscular junctions of *Xenopus* embryos transiently expressing either human AChE or mouse nAChR. Part of the transgenic NMJs grew to sizes unobserved in control embryos, accommodated more AChE within the synaptic cleft, and displayed enhanced staining for AChE activity within nerve terminals. These changes were significantly more conspicuous at 21°C (this report) than at 17°C (10, 11), as would be expected based on the mammalian origin of the transgenes (17, 18). Therefore, although the receptor initiates neurotransmission and the enzyme terminates it, overexpression of either protein enhanced the development of *Xenopus* NMJs. The fact that both these proteins mediate the physiological effects of acetylcholine suggests a trophic role for ACh in NMJ development.

We were able to detect significant increases in the abundance of nAChR in extracts of animals transiently transgenic for human AChE. This result correlates overexpression of endogenous nAChR with overexpression of exogenous AChE. In contrast, we were unable to detect increases in esterase activity in whole cell extracts of animals transiently transgenic for mouse nAChR, possibly because of the wide tissue distribution of AChE in *Xenopus* embryos (19), which masks the NMJ differences. Nevertheless, ultrastructural analyses demonstrated changes in the expression of AChE within NMJs of nAChR transgenic embryos. These observations imply coordinated expression of AChE and AChR during NMJ formation.

Most of the nerve labeling in NMJs from microinjected embryos could be attributed to the expression of transgenes. Thus, we were able to examine a subgroup of NMJs (hAChE transgenics labeled in their nerve terminals) in which 70% received synaptic input from a nerve expressing exogenous esterase. Within this subgroup, uncertainty introduced by mosaic expression was reduced and transgene-dependent differences were enhanced.

Nerve terminal expression of AChE appeared to be one of the features characterizing the large NMJs particular to the transgenic animals. In hAChE transgenics, apparently higher levels of AChE were observed in the synaptic cleft of NMJs labeled presynaptically than in those devoid of nerve-terminal staining. This difference was not observed for NMJs from either control or nAChR transgenic embryos. Thus, the synaptic accumulation of endogenous *Xenopus* AChE was tightly linked to postsynaptic length regardless of its nerve or muscle origin(s). In contrast, neuronal AChE expression in animals transgenic for the human enzyme induced synaptic accumulation of AChE in a manner less subject to host regulation. These observations are consistent with findings demonstrating neuronal contribution of AChE to the synaptic cleft in adult *Xenopus* NMJs (20). They also highlight a putative role for muscle AChE in establishing NMJ length as opposed to a neuronal influence on the width of the synaptic cleft.

The question of whether or not ACh exerts trophic effects on muscle was previously approached by stimulation under

toxin-mediated suppression of ACh release (reviewed in refs. 3 and 6). However, AChE is the principal agent controlling ACh hydrolysis in NMJs (1, 21). Therefore, AChE overexpression should decrease ACh levels and, consequently, postsynaptic signals—i.e., ion currents, depolarization, or both. In response, affected cells appeared to upregulate nAChR. Increased nAChR could potentially overcome the reduced signal and restore appropriate functioning. Under these conditions, spatial constraints on receptor density (22) might enforce a concomitant increase in other NMJ components, leading to synapse enlargement and accommodation of the excess molecules.

nAChR expressed in *Xenopus* oocytes is correctly assembled, transported to, and inserted into the plasma membrane in a physiologically functional form (12). Therefore, NMJs overexpressing exogenous nAChR should increase in length to the same extent as AChE-overexpressing ones. Since ACh is released in excess amounts (2, 23), the postsynaptic signal in such NMJs would also be enhanced. In response, the amphibian system was found to increase AChE expression within the synapse, which can suppress the augmented signal down to levels compatible with normal functioning. Thus, a partially overlapping flow of feedback responses eventually leads to enhancement of NMJ development in both cases.

The NMJ cross-section parameters displaying developmental plasticity included postsynaptic length, AChE accumulation, and width of the synaptic cleft. Previous cell culture studies demonstrated modulation of part of these parameters by manipulation of key structural proteins such as agrin (24) or synapsin (25). Our present *in vivo* studies suggest that all of these NMJ properties are responsive to ACh levels and therefore subject to modulation through heterologous expression of key cholinergic proteins. Thus, microinjected *Xenopus* embryos could be used, together with mRNA amplification techniques such as differential PCR display (26), to clone and characterize yet unknown genes whose expression is modified during changes in NMJ development.

This work was supported by the USA–Israel Binational Science Foundation (to H.S. and J.P.) and the Israel Academy of Sciences (to H.S.).

1. Hall, Z. W. & Sanes, J. R. (1993) *Cell* **72**/*Neuron* **10** (Suppl.), 99–121.
2. Anglister, L., Stiles, J. R. & Salpeter, M. M. (1994) *Neuron* **12**, 783–794.
3. Tucek, S. (1990) *Prog. Brain Res.* **84**, 467–477.
4. Jennekens, F. G. I., Hesselmans, L. F. G. M., Veldman, H., Jansen, E. N. H., Spaans, F. & Molenaar, P. C. (1992) *Muscle Nerve* **15**, 63–72.
5. Lauder, J. M. (1993) *Trends Neurosci.* **16**, 233–240.
6. Laufer, R. & Changeux, J. P. (1989) *Mol. Neurobiol.* **3**, 1–53.
7. Jennings, C. G. B. & Burden, S. J. (1993) *Curr. Opin. Neurobiol.* **3**, 75–81.
8. Alfonso, A., Grundahl, J. S., Han, H. P. & Rand, J. B. (1993) *Science* **261**, 617–619.
9. Wyttenbach, C. R. & Thompson, S. C. (1985) *Am. J. Anat.* **174**, 187–202.
10. Ben Aziz-Aloya, R., Seidman, S., Timberg, R., Sternfeld, M., Zakut, H. & Soreq, H. (1993) *Proc. Natl. Acad. Sci. USA* **90**, 2471–2475.
11. Seidman, S., Ben Aziz-Aloya, R., Timberg, R., Loewenstein, Y., Velan, B., Shafferman, A., Liao, J., Norgaard-Pedersen, B., Brodbeck, U. & Soreq, H. (1994) *J. Neurochem.* **62**, 1670–1681.
12. Patrick, J., Boulter, J., Goldman, D., Gardner, P. & Heinemann, S. (1986) *Ann. N.Y. Acad. Sci.* **505**, 194–207.
13. Seed, B. (1987) *Nature (London)* **329**, 840–842.
14. Quinn, A., Harrison, R., Jehanli, A. M. T., Lunt, G. G. & Walsh, S. (1988) *J. Immunol. Methods* **107**, 197–203.
15. Neville, L. F., Gnatt, A., Loewenstein, Y., Seidman, S., Ehrlich, G. & Soreq, H. (1992) *EMBO J.* **11**, 1641–1649.
16. Vize, P. D., Melton, D. A., Hemmati-Brivanlou, A. & Harland, R. M. (1991) *Methods Cell Biol.* **36**, 367–387.
17. Soreq, H. & Seidman, S. (1992) *Methods Enzymol.* **207**, 225–265.
18. Duval, N., Massoulie, J. & Bon, S. (1992) *J. Cell Biol.* **118**, 641–653.
19. Cohen, M. W. (1980) *J. Exp. Biol.* **89**, 43–56.
20. Anglister, L. & McMahan, U. J. (1985) *J. Cell Biol.* **101**, 735–743.
21. Changeux, J. P. (1991) *New Biol.* **3**, 413–429.
22. Salpeter, M. & Loring, R. H. (1985) *Prog. Neurobiol.* **25**, 297–325.
23. Matthews-Bellinger, U. & Salpeter, M. (1978) *J. Physiol. (London)* **279**, 297–313.
24. McMahan, U. J. (1990) *Cold Spring Harbor Symp. Quant. Biol.* **55**, 407–418.
25. Han, H. Q., Nichols, R. A., Rubin, M. R., Bahler, M. & Greengard, P. (1991) *Nature (London)* **349**, 697–700.
26. Liang, P. & Pardee, A. (1992) *Science* **257**, 967–971.